Cycloaddition and Nucleophilic Substitution Reactions of the Monomeric Titanocene Sulfido Complex (η^5-$C_5Me_5)_2(C_5H_5N)Ti{=}S$

Zachary K. Sweeney, Jennifer L. Polse, Richard A. Andersen,* and Robert G. Bergman*

Contribution from the Department of Chemistry, University of California, Berkeley, California 94720

Received March 16, 1998

Abstract: The titanocene sulfido complex $Cp^*_2(py)Ti{=}S$ (**1**, py = pyridine) reacts reversibly with terminal alkynes to give the thiametallacyclobutenes $Cp^*_2Ti(SC(R){=}CH)$ (R = H (**2**), Ph (**3**), Tol (**4**), TMS (**5**)). Complex **1** also reacts with alkyl halides to give products derived from formal 1,2-addition across the titanium−sulfur bond. Treatment of **1** with allyl halides results in the formation of $Cp^*_2Ti(X)SCH_2CHCH_2$ (X = Cl (**10**), F (**16**), Br (**17**), I (**18**)). Reaction of **1** with alkyl-substituted allyl chlorides showed that displacement of the halide anion occurs with S_N2' regiochemistry. A kinetic study of the conversion of **1** to **10** is consistent with a mechanism in which pyridine dissociation from the metal center precedes reaction of allyl chloride with the $Cp^*_2Ti{=}S$ fragment. The S_N2' regiochemistry of the reaction is explained by postulating coordination of the halogen atom to the metal center in the reaction transition state. Complex **1** also reacts with allyl tosylate, but labeling experiments show (in contrast to the allyl chloride reaction) that substitution of the tosylate functionality occurs via a S_N2 pathway. Heterocycles formed from the reaction of **1** with α,β-unsaturated aldehydes were also isolated and characterized.

Introduction

In contrast to the inertness of many transition metal multiple bonds,[1] the M=X (X = O, NR, S, PR) linkage in titanocene and zirconocene complexes is unusually reactive. A wide range of transformations has now been established for these complexes, including overall [2 + 2] cycloadditions with olefins,[2,3] alkynes,[4−7] imines,[8] and carbonyls[9] and C−H[10] and H−H[11] bond cleavage reactions with hydrocarbons and dihydrogen.[12]

In an attempt to extend this chemistry to titanium−sulfur multiple bonds, we recently synthesized $Cp^*_2(py)Ti{=}S$ (**1**, Cp* = η^5-C_5Me_5) and studied its reactivity toward dihydrogen and silanes.[13] We have now found that the Ti=S bond in **1** exhibits cycloaddition reactivity, and in this paper we report the regioselective reactions of **1** with alkynes and nitriles. In addition, we have investigated the nucleophilicity of **1** and have found that this complex undergoes an especially regioselective series of S_N2' substitution reactions with allyl chlorides.

Scheme 1

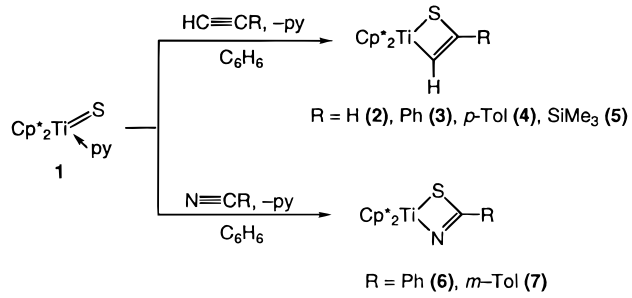

Results

Reactions of 1 with Terminal Alkynes and Nitriles. Although no reaction occurs when **1** is treated with diphenylacetylene, the sulfido complex reacts with terminal alkynes at room temperature over a period of several hours to give the orange thiametallacyclobutenes **2**−**5** (Scheme 1) in good yield. In all cases the ^{1}H NMR spectrum of the product shows only one Cp* resonance, suggesting that a single regioisomer has been formed in the reaction. Attempts to determine the regiochemistry of the cycloaddition by hydrolysis of the metallacycle to the corresponding ketones with dilute aqueous HCl[5] led to the formation of several products (as determined by GC analysis). However, the large downfield shifts of the alkynyl protons in the ^{1}H NMR spectra of **2**−**5** (to between 8.5 and 7.8 ppm) and the appearance of methine carbon resonances between 220 and 190 ppm in the $^{13}C\{^1H\}$ NMR spectra of these products are consistent with formation of thiametallacyclobutene compounds in which the terminal methine carbon is bound to titanium.

To further confirm the regiochemistry of these cycloadditions, a single-crystal X-ray diffraction study of **5** was performed. Crystal and data collection parameters are shown in Table 1, and details of the structure determination are given in the Experimental Section and as Supporting Information. An ORTEP diagram of **5** is presented in Figure 1, and selected bond

(1) Nugent, W. A.; Mayer, J. M. *Metal−Ligand Multiple Bonds*; John Wiley and Sons: New York, 1988.
(2) Walsh, P. J.; Hollander, F. J.; Bergman, R. G. *Organometallics* **1993**, *12*, 3705.
(3) Schwartz, D. J.; Smith, M. R.; Andersen, R. A. *Organometallics* **1996**, *15*, 1446.
(4) Walsh, P. J.; Baranger, A. M.; Bergman, R. G. *J. Am. Chem. Soc.* **1992**, *114*, 1708.
(5) Baranger, A. M.; Walsh, P. J.; Bergman, R. G. *J. Am. Chem. Soc.* **1993**, *115*, 2753.
(6) Lee, S.; Bergman, R. G. *Tetrahedron* **1995**, *51*, 4255.
(7) Carney, M. J.; Walsh, P. J.; Hollander, F. J.; Bergman, R. G. *Organometallics* **1992**, *11*, 761.
(8) Meyer, K. E.; Walsh, P. J.; Bergman, R. G. *J. Am. Chem. Soc.* **1995**, *117*, 974.
(9) Lee, S. Y.; Bergman, R. G. *J. Am. Chem. Soc.* **1996**, *118*, 6396.
(10) Lee, S. Y.; Bergman, R. G. *J. Am. Chem. Soc.* **1995**, *117*, 5877.
(11) Howard, W. A.; Trnka, T. M.; Waters, M.; Parkin, G. *J. Organomet. Chem.* **1997**, *528*, 95.
(12) For leading references to reactive early-metal nonmetallocene imido complexes see: Bennett, J.; Wolczanski, P. *J. Am. Chem. Soc.* **1997**, *119*, 10696.
(13) Sweeney, Z. K.; Polse, J. L.; Andersen, R. A.; Bergman, R. G.; Kubinec, M. G. *J. Am. Chem. Soc.* **1997**, *119*, 4543.

S0002-7863(98)00877-4 CCC: $15.00
Published on Web 07/23/1998

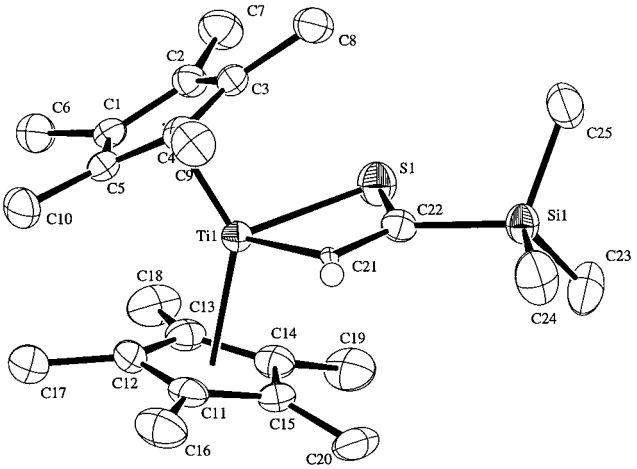

Figure 1. ORTEP diagram of $Cp^*_2Ti(SC(Si(CH_3)_3)CH)$ (**5**).

Table 1. Crystal Data for **5**, **14**, and **21**

	compd		
	5	**14**	**21**
formula	$C_{25}H_{40}SSiTi$	$C_{25}H_{39}ClSTi$	$C_{30}H_{40}OSTi$
a (Å)	9.2973(2)	9.5053(1)	9.6350(5)
b (Å)	18.24120(10)	16.9754(3)	10.8004(6)
c (Å)	14.7021(3)	15.0822(3)	25.828(1)
β (deg)	95.212(1)	100.797(1)	100.724(1)
V (Å^3)	2483.08(6)	2390.53(6)	2640.8(2)
μ(Mo Kα) (cm^{-1})	5.66	5.66	4.23
space group	$P2_1/c$	$P2_1/c$	$P2_1/c$
T (°C)	−100	−93	−99
reflns collcd	11 074	11 366	10 623
unique reflns	4534	4317	3989
obsd reflns	2713	2416	2635
$I > 3.00\sigma(I)$ var	253	253	298
reflns/param	10.72	9.55	8.84
R	0.049	0.049	0.033
R_w	0.056	0.055	0.040
goodness of fit	1.89	1.65	1.47
p-factor	0.030	0.030	0.030

Table 2. Selected Bond Distances (Å) and Angles (deg) for **5**

bond	dist	bond	angle
Ti−S	2.403(1)	S−Ti−C21	78.0(1)
Ti−C21	2.157(5)	Ti−S−C22	71.6(1)
S−C22	1.840(4)	S−C22−C21	123.2
C21−C22	1.423(6)	Ti−C21−C22	87.1(3)
Ti−Cp1	2.118	S−C22−Si	112.3(2)
Ti−Cp2	2.116	Si−C22−C21	124.6(3)

lengths and bond angles are shown in Table 2. The trimethylsilyl group is indeed located as far as possible from the sterically demanding Cp* ligands. Other structural features are similar to those of previously characterized metallacyclobutenes. For example, the Ti−C21 bond length of 2.157(5) Å is close to the titanium−carbon bond length of 2.144(1) Å in the related oxametallacycle $Cp^*_2Ti(OC(Ph)=CH)$,[14] and the Ti−S−C bond angle of 71.6(1)° is similar to the Zr−S−C bond angle in $Cp^*_2Zr(SC(Ph)=CPh)$ (74.2(2)°).[7]

As was observed with the related oxo complexes and their cycloadducts, the thiametallacyclobutenes were found to exchange alkyne fragments when heated in the presence of a second alkyne.[5,14,15] For example, heating phenylacetylene adduct **3** to 75 °C in benzene in the presence of 1 equiv of *p*-tolylacetylene resulted in the formation of a mixture of **3** and **4** (as determined by ^{1}H NMR spectroscopy). Although we have not investigated the mechanism of the alkyne exchange process in this system, we assume that it involves initial cycloreversion of the metallacycle to $[Cp^*_2Ti{=}S]$ followed by reaction of this intermediate with another alkyne.[16]

Scheme 2

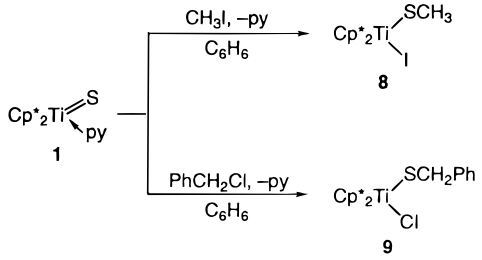

Interestingly, metallacycles **2**−**5** were thermally stable when heated in the absence of added alkyne in benzene at 105 °C for 24 h. These results contrast with the thermal chemistry of the analogous oxametallacylobutenes, which rearrange to hydroxy−acetylide complexes upon thermolysis.[14] This difference is especially pronounced in a comparison of the reactivity of **1** and $Cp^*_2(py)Ti{=}O$ toward (trimethylsilyl)acetylene. Compound **1** reacts with (trimethylsilyl)acetylene to form thermally stable **5**, while treatment of $Cp^*_2(py)Ti{=}O$ with (trimethylsilyl)-acetylene at room temperature results in the quantitative formation of the hydroxy−acetylide complex $Cp^*_2Ti(OH)$-$CCSiMe_3$.[15]

Reaction of **1** with an excess of benzonitrile or tolunitrile results in conversion to products that are tentatively identified as the four-membered metallacycles **6** and **7** (Scheme 1). The NMR spectra of these compounds, as well as elemental analysis and mass spectral information, indicate that further insertion of a nitrile to form six-membered metallacycles (incorporating 2 equiv of benzonitrile) does not occur. Formation of a six-membered metallacycle was observed when $Cp^*_2(py)Zr{=}S$ was treated with excess benzonitrile, although a four-membered metallacycle resulting from reaction of the zirconium−sulfido complex with 1 equiv of benzonitrile was postulated as an intermediate in this transformation.[7] The bound nitriles in **6** and **7** can be replaced with other nitriles or silanes. Thus, treatment of a benzene solution of **6** with 2 equiv of *m*-tolunitrile gives a mixture of **6** and **7**, and reaction of **6** with H_2SiMe_2 produces $Cp^*_2Ti(H)SSiHMe_2$ [13] and free benzonitrile, as identified by ^{1}H NMR spectroscopy.

Reaction of 1 with Organic Halides. We have found that **1** reacts cleanly with a number of organic halides to give products resulting from formal 1,2-addition across the titanium−sulfur bond. Addition of methyl iodide to a benzene solution of **1** results in a color change from red to brown and formation of $Cp^*_2Ti(I)SCH_3$ (**8**), isolated in 55% yield (Scheme 2). This product is identified in the ^{1}H NMR spectrum by two singlets corresponding to the Cp* and SCH_3 protons. The mass spectrum of **8** shows the molecular ion and a base peak corresponding to loss of the SCH_3 fragment. Similarly, reaction of **1** with benzyl chloride results in formation of $Cp^*_2Ti(Cl)$-$SCH_2C_6H_5$ (**9**), isolated in 78% yield. The $^{13}C\{^1H\}$ NMR spectrum of **9** includes a single methylene signal at 48.7 ppm assigned to the benzylic methylene carbon, and the mass spectrum shows a molecular ion and a peak corresponding to loss of $SCH_2C_6H_5$. Attempts to investigate the mechanism of the reaction of **1** and benzyl chloride were complicated by the

(14) Polse, J. L.; Andersen, R. A.; Bergman, R. G. *J. Am. Chem. Soc.* **1995**, *117*, 5393.

(15) Polse, J. L.; Andersen, R. A.; Bergman, R. G. Manuscript in preparation.

(16) Exchange of the alkyne fragment of the analagous oxametallacyclobutenes was also explained by initial cycloreversion of the metallacycles. See ref 14.

Scheme 3

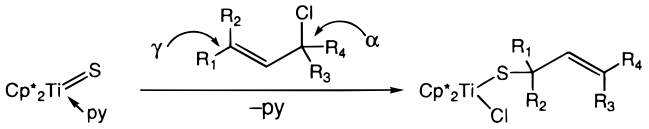

Cmpd	R1	R2	R3	R4
10	H	H	H	H
11	H	H	Me	H
12	Me	H	H	H
13	H	H	Me	Me
14	Me	Me	H	H

Scheme 4

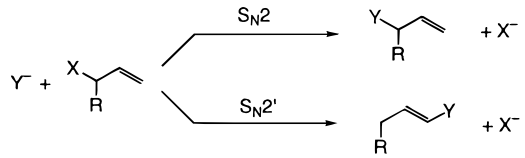

gradual decomposition of the product in the presence of excess benzyl chloride. However, several experiments in which the reaction was monitored by UV−visible spectroscopy indicate that the reaction rate is inhibited by increasing pyridine concentration (vide infra).

No reaction is observed when **1** is treated with allyl ethyl ether or allyl acetate. However, addition of allyl chloride to a benzene solution of **1** results in an immediate color change from red to blue and clean formation of **10** (Scheme 3). This compound was isolated as blue crystals from cold toluene/pentane and showed peaks in the ^{1}H NMR spectrum consistent with the presence of an allyl functionality. No intermediates were observed when the reaction was monitored by NMR spectroscopy at −30 °C.

To determine if **1** reacts with allyl chlorides in an S_N2 or S_N2' fashion[17] (Scheme 4), **1** was treated with several substituted allyl chlorides. All of these reactions were essentially quantitative (≥95% as judged by ^{1}H NMR spectroscopy), and in most cases the products could be isolated in good yield as blue crystals. To our surprise, analysis of the products of these reactions indicated that *substitution takes place exclusively in an S_N2'* fashion, independent of the substituents on the allyl chloride. The products of reactions with isomeric allyl chlorides are easily distinguished by their ^{1}H NMR spectra. For example, the ^{1}H NMR spectrum of **14** shows a single methyl resonance integrating to 6 protons at 1.68 ppm, while the ^{1}H NMR spectrum of **13** shows two methyl resonances assigned to the cis and trans methyl groups at 1.70 and 1.66 ppm. The products can also be distinguished by their different thermal stability. Compound **14**, in which the sulfur atom is connected to a tertiary carbon, decomposes to a number of unidentified products over several hours in solution at 20 °C, while isomer **13** is stable for several days under the same conditions.

As a final test of the selectivity of these substitution reactions, **1** was treated with 1-chloro-2,4-pentadiene (Scheme 5). The ^{1}H and ^{13}C NMR spectra of the product of this reaction clearly show that the sulfido ligand reacts exclusively at the γ-position of the dienyl chloride. In particular, the ^{13}C{^{1}H} NMR spectrum of **15** shows only 3 resonances for the C_s-symmetric thiolate ligand. This result provides further evidence of the preference for γ-substitution in this system, since either S_N2 or S_N2'' substitution would result in formation of a *n*-pentadienethiolate ligand.

(17) DeWolfe, R. H.; Young, W. G. *Chem. Rev.* **1956**, *56*, 753.

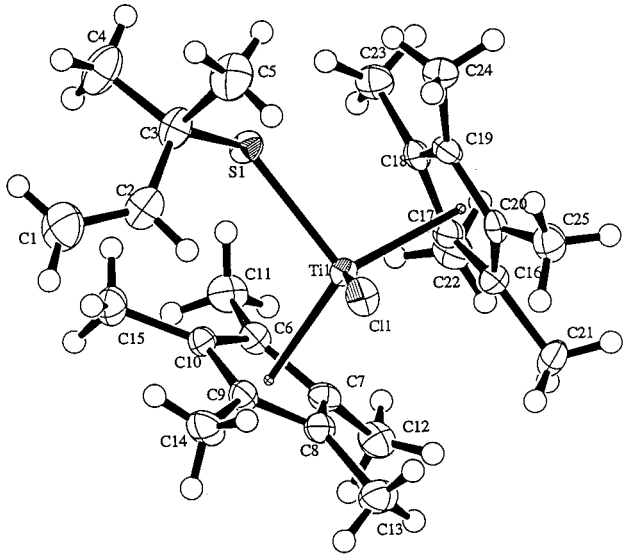

Figure 2. ORTEP diagram of Cp*$_2$Ti(Cl)SC(CH$_3$)$_2$CHCH$_2$ (**14**).

Scheme 5

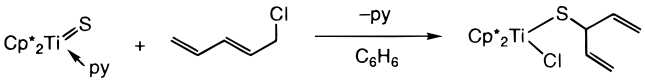

1 **15**

Table 3. Selected Bond Distances (Å) and Angles (deg) for **14**

bond	dist	bond	angle
Ti−S	2.444(2)	Cl−Ti−S	95.69(6)
Ti−Cl	2.346(2)	Ti−S−C3	124.1(2)
C1−C2	1.314(8)	Cp1-Ti−Cp2	134.5
Ti−Cp1	2.140	C3−C2−C1	126.3(5)
Ti−Cp2	2.146	S1−Ti−Cp1	108.4
C2−C3	1.489(7)	S1−Ti−Cp2	100.9

To further confirm that substitution occurred in an S_N2' manner, a single-crystal X-ray diffraction study of **14** was performed. An ORTEP diagram of **14** is shown in Figure 2, and Table 3 provides intramolecular bond lengths and angles. As expected, the structure shows that attack of the sulfido ligand has occurred at the electronically and sterically disfavored γ-position. The double bond in the product is localized between the terminal carbons of the allyl fragment (C1−C2 = 1.314(8) Å), and the −SC(CH$_3$)$_2$CH=CH$_2$ ligand is oriented at an angle that minimizes unfavorable steric interaction with the Cp* ligands. Although the orientation of this ligand makes the Cp* ligands inequivalent in the solid state, the presence of a single Cp* resonance in the ^{1}H NMR spectrum indicates that the ligand rotates rapidly in solution.

A kinetic study of the reaction between **1** and allyl chloride was performed in order to gain further insight into the mechanism of these unusual substitution reactions. Production of **10** was followed by UV−visible spectroscopy. In the presence of excess pyridine and allyl chloride, good pseudo-first-order rate behavior was observed. The change in the pseudo-first-order rate constants k_{obs} with respect to the concentration of pyridine was studied at constant concentrations of **1** and allyl chloride.[18] A plot of $1/k_{obs}$ versus [py]/[allyl chloride] is shown in Figure 3. A linear fit of the data has a goodness-of-fit factor of 0.993.

Reaction of **1** with allyl halides appears to be quite general. Substitution reactions also occurred when **1** was treated with

(18) Details of the kinetic study are provided as Supporting Information.

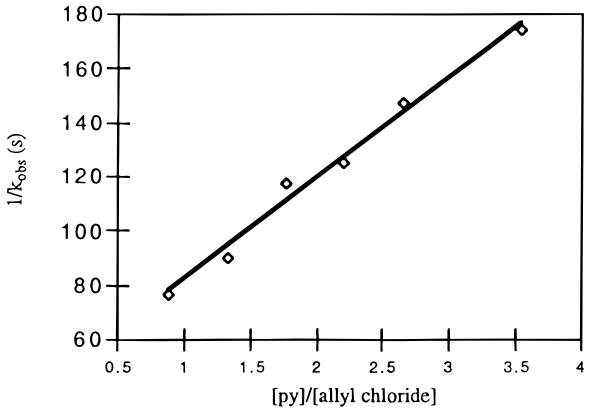

Figure 3. Plot of $1/k_{obs}$ vs [py]/[allyl chloride] for the reaction of **1** with allyl chloride.

Scheme 6

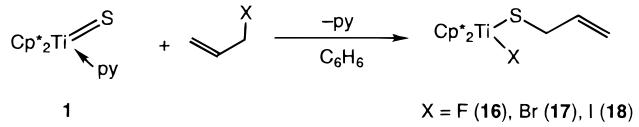

1 X = F (**16**), Br (**17**), I (**18**)

Table 4. ^{1}H NMR Chemical Shift Data for $Cp^*_2Ti(X)SCH^aCH^b{=}C(H^c)H^d$

cmpd	X	$\delta(H)^a$	$\delta(H)^b$	$\delta(H)^c$	$\delta(H)^d$
16	F	3.53	6.16	4.97	5.20
10	Cl	3.76	6.13	4.95	5.19
17	Br	3.82	6.13	4.95	5.18
18	I	3.90	6.15	4.95	5.18
19	OTs	4.72	6.45	5.10	5.35

Scheme 7

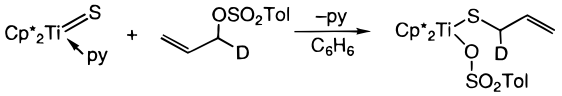

1 **19-d**

allyl fluoride, allyl bromide, or allyl iodide (Scheme 6). The product of each of these reactions was isolated and characterized (see Experimental Section for details). The reaction of **1** with allyl fluoride is significantly slower than the reaction of **1** with other allyl halides. Competition reactions between **1** and equimolar amounts of allyl bromide and allyl chloride indicate that the reaction of **1** with allyl bromide occurs approximately five times more rapidly than the reaction of **1** with allyl chloride.

Reactivity of 1 toward Allyl *p*-Toluenesulfonate. To determine if the regioselectivity observed in the reactions of **1** with allyl chlorides was dependent on the halide functionality, **1** was treated with allyl tosylate to form compound **19** (Scheme 7). In sharp contrast to the reactions of **1** with allyl chlorides, which are complete in minutes, the tosylate reaction requires several days at 20 °C to go to completion. The similarities between the ^{1}H and $^{13}C\{^1H\}$ NMR spectra of **19** and **10** and **16**−**18** (Table 4) suggest that **19** has the same connectivity as its halogenated analogues. The regiochemistry of this substitution was probed by treating **1** with allyl tosylate-1-*d*, and the product of this reaction (**19-*d***) was analyzed by NMR spectroscopy. The ^{1}H, ^{2}H, and $^{13}C\{^1H\}$ spectra clearly show that reaction takes place predominately in an *S_N2 fashion* (Scheme 7). In particular, the ^{2}H spectrum of the product in C_6H_6 shows only a single signal at 4.7 ppm, and the $^{13}C\{^1H\}$ spectrum, which was otherwise identical to the fully protiated analogue, shows a 1:1:1 triplet instead of a singlet at 44 ppm.

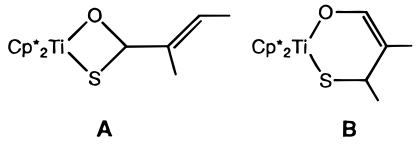

Figure 4. Possible products of the reaction of **1** with 2-methyl-2-butenal.

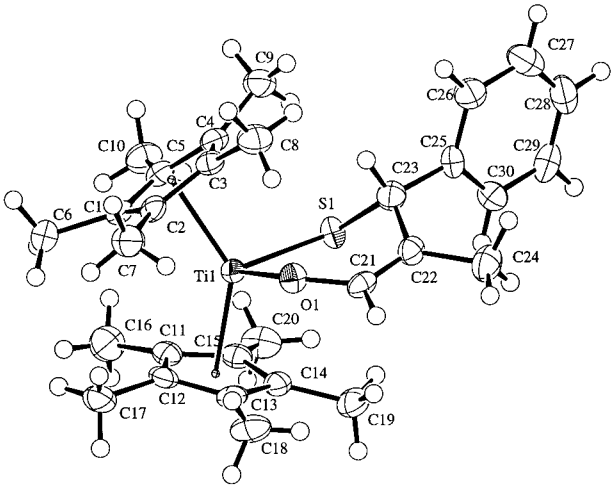

Figure 5. ORTEP diagram of $Cp^*_2Ti(SC(Ph)HC(Me)C(H)O)$ (**21**).

Scheme 8

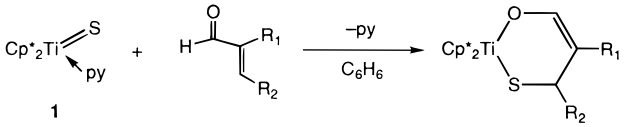

1

20: R_1 = Me, R_2 = Me
21: R_1 = Me, R_2 = Ph

Reactions of 1 with α,β-Unsaturated Aldehydes. To determine whether the γ-attack observed in the reaction of **1** with allyl halides could be generalized to other organic reactants, the sulfido complex was treated with α,β-unsaturated aldehydes. These reactions led to the six-membered cyclic products **20** and **21** shown in Scheme 8. Important features of the ^{1}H NMR spectra of these products are two resonances corresponding to diastereotopic Cp* protons and a large upfield shift of the formerly aldehydic proton. To distinguish between products arising from overall [2 + 2] and [4 + 2] cycloadditions (illustrated as A and B in Figure 4), a ^{1}H−^{13}C HMQC NMR study[19] of **20** was performed. The results indicate that the hydrogen adjacent to a methyl group, which appears as a quartet at 4.15 ppm in the ^{1}H NMR spectrum, is connected to a carbon that appears at 43.2 ppm in the $^{13}C\{^1H\}$ NMR spectrum. This strongly suggests that this carbon is sp^3 hybridized and that the structure of the product is the six-membered metallacycle (type B in Figure 4). To further confirm this conclusion, the structure of **21** was determined by X-ray crystallography. Crystal and data collection parameters are shown in Table 1, and details of the structure determination are given in the Experimental Section. An ORTEP diagram of **21** is shown in Figure 5, and Table 5 provides intramolecular bond lengths and bond angles. The structure shows that the titanium−sulfur and titanium−oxygen bond lengths are in the range expected for Ti−S and Ti−O single bonds. The six-membered ring is strongly puckered, and the phenyl group resides in an equatorial position.

(19) Bax, A.; Subramanian, S. *J. Magn. Reson.* **1986**, *67*, 565.

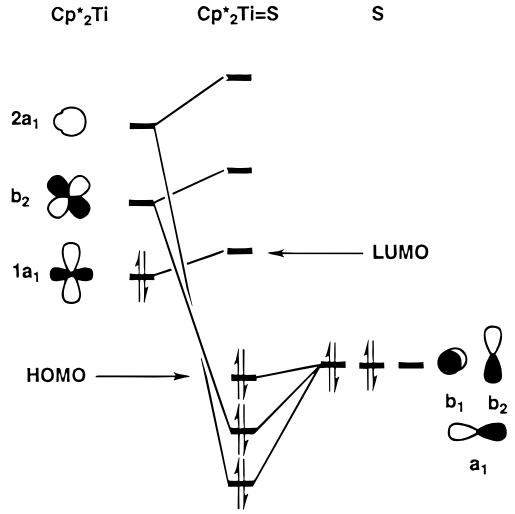

Figure 6. Molecular orbital diagram showing the frontier orbitals of $Cp^*_2Ti{=}S$.

Table 5. Selected Bond Distances (Å) and Angles (deg) for **21**

bond	dist	bond	angle
Ti−S	2.4231(9)	S−Ti−O	87.70(6)
Ti−O	1.890(2)	S−C23−C22	111.6(2)
C22−C21	1.319(4)	C23−C22−C21	119.6(2)
C22−C23	1.532(4)	C22−C21−O	125.4(3)
S−C23	1.857(3)	C21−O−Ti	137.3(2)
O−C21	1.350(3)	C23−S−Ti	102.7(1)
Ti−Cp1	2.151	O−Ti−Cp1	103.7
Ti−Cp2	2.136	S−Ti−Cp1	107.3

Discussion

The synthesis and structure of $Cp^*_2Ti(S)py$ (**1**) have been reported in preliminary form.[13] The pyridine ligand in this complex is labile in solution and is rapidly displaced by stronger-binding ligands such as *p*-(dimethylamino)pyridine. Dissociation of pyridine from the 18-electron complex[20] results in formation of a coordinatively unsaturated 16-electron molecule that contains a vacant metal-based orbital perpendicular to the metal−sulfur bond.[21] Calculations on the cyclopentadiene analogue of this compound using ab initio methods predict that the Ti−S bond polarity expected from the electronegativity difference between the sulfur ligand and the metallocene fragment is offset somewhat by π donation from the ligand to the metal center and that the bond is best described as covalent.[22] A simple molecular orbital diagram showing the frontier orbital configuration of $Cp^*_2Ti{=}S$ is illustrated in Figure 6.

We have found that **1** readily forms metallacycles when treated with alkynes and nitriles. The regiochemistry of the alkyne cyclization reaction appears to be controlled by steric factors. Complex **1**, like the closely related oxo compound $Cp^*_2Ti(O)py$, reacts with terminal alkynes to place the alkyne substituent in the β position, away from the sterically demanding Cp^*_2Ti center. The ready reversibility of these cyclization reactions has also been observed in the analogous oxo system. However, the oxatitanacyclobutenes rearrange to the corresponding hydroxy−acetylide complexes upon thermolysis (eq 1).[14]

Similar conversion of the thiametallacyclobutenes to hydrosulfido acetylide compounds would produce a relatively weak SH bond. Because of this, we suspect that rearrangement is not observed because the thiametallacylclobutenes are thermodynamically more stable than their hydrosulfido−acetylide isomers.

The detailed mechanism of cycloaddition reactions between $Cp_2M{=}X$ complexes (M = Ti, Zr; X = CR_2, NR, O, S) and alkynes and alkenes is now well understood. Previous workers in our group have shown that the reaction of a zirconocene imido pyridine complex with diphenylacetylene is preceded by pyridine dissociation (eq 2).[6]

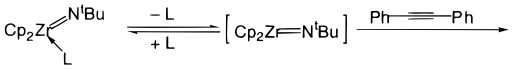

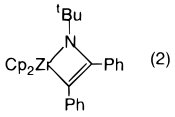

As mentioned above, dissociation of the labile ligand from the metal center releases a metal-based orbital adjacent to the reactive metal−heteroatom bond. Norton et al. have recently suggested that apparent [2 + 2] organometallic cycloadditions always involve initial coordination of one partner to the metal,[23] and we believe that ligand dissociation is required in order for the above-mentioned cyclization reactions to occur because they are mediated by this available empty orbital. This postulate is consistent with the calculations of Upton and Rappé, who studied the formation of titanacyclobutanes from olefins and titanium alkylidene complexes.[24] An empty metal-based orbital adjacent to the reactive ligand is also thought to participate in the hydrogenation[25] and dealkylation[26] reactions of d^0 metal−carbon bonds.

The apparent nucleophilicity of early metal complexes containing metal−ligand multiple bonds is generally thought to be a consequence of the high energy of the metal frontier orbitals.[1] The resulting localization of electron density on the ligand enables some of these complexes to form metallacycles with heterocumulenes or simple adducts with strong Lewis acids. For example, Geoffroy et al. found that (tmtaa)Ti=S reacts with perfluorinated acetone,[27] and Green et al.[28] and Floriani et al.[29] have recently characterized adducts formed from the reaction of titanium oxo complexes with boranes.[30−38] However, as mentioned above, theoretical calculations have shown that the Ti=S bond in $Cp_2Ti(S)$ is probably best described as covalent, and we were surprised by the facility with which **1** underwent nucleophilic substitution reactions with alkyl halides. Since we were interested in the possibility that the metal might interact

(20) Parkin and Bercaw have proposed that 18 electron complexes of this type be referred to as "class b" complexes. See: Parkin, G.; Bercaw, J. E. *J. Am. Chem. Soc.* **1989**, *111*, 391.

(21) Lauher, J. W.; Hoffman, R. *J. Am. Chem. Soc.* **1976**, *98*, 1729.

(22) Fischer, J. M.; Piers, W. E.; Ziegler, T.; MacGillivray, L. R.; Zaworotko, M. J. *Chem. Eur. J.* **1996**, *2*, 1221.

(23) Bender, B. R.; Ramage, D. L.; Norton, J. R.; Wiser, D. C.; Rappé, A. K. *J. Am. Chem. Soc.* **1997**, *119*, 5628.

(24) Upton, T. H.; Rappé, A. K. *J. Am. Chem. Soc.* **1985**, *107*, 1206.

(25) Gell, K. I.; Posin, B.; Schwartz, J.; Williams, G. M. *J. Am. Chem. Soc.* **1982**, *104*, 1846.

(26) Caulton, K. G.; Marsella, J. A. *J. Am. Chem. Soc.* **1982**, *104*, 2361.

(27) Housmekerides, C. E.; Ramage, D. L.; Kretz, C. M.; Shontz, J. T.; Geoffroy, G. L. *Inorg. Chem.* **1992**, *31*, 4453. tmtaa = dianion of 7, 16-dihydro-6,8,15,17-tetramethyldibenzo[*b*,*i*][1,4,8,11]tetraazacyclotetradecane.

(28) Galsworthy, J. R.; Green, M. L. H.; Muller, M.; Prout, K. *J. Chem. Soc., Dalton Trans.* **1997**, 1309.

(29) Franceschi, F.; Gallo, E.; Solari, E.; Floriani, C.; Chiesi-Villa, A.; Rizzoli, C.; Re, N.; Sgamellotti, A. *Chem. Eur. J.* **1996**, *2*, 1466.

Scheme 9

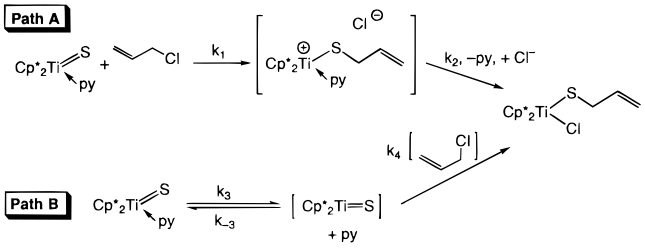

with the leaving group in the transition state of these substitution reactions, we have examined the origins of the apparent nucleophilicity of **1** more closely.

It is likely that pyridine coordination to the metal center indirectly increases the electron density on the sulfur ligand by increasing the electron density at the metal center. Since this might affect the nucleophilic reactivity of the sulfido ligand, we attempted to determine whether reactions in which **1** functions as a nucleophile occur directly from the pyridine-bound complex or whether prior dissociation of pyridine is required. Two general mechanisms through which **1** might react as a nucleophile toward allyl chloride are shown in Scheme 9. Path A involves direct nucleophilic attack of the sulfur atom of the pyridine-bound complex followed by cation−anion recombination and liberation of pyridine. In path B, initial rapid and reversible pyridine dissociation generates an unsaturated complex that reacts with allyl chloride in a subsequent step.[39]

The observed rate constant for the associative reaction (path A) should be zero order in pyridine concentration and directly proportional to the concentration of allyl chloride (eq 3). When

$$\text{rate} = k_1[\text{RCl}][\mathbf{1}] = k_{\text{obs}}[\mathbf{1}] \tag{3}$$

$$k_{\text{obs}} \propto [\text{RCl}] \tag{4}$$

k_{obs} is measured under pseudo-first-order conditions in the presence of different concentrations of allyl chloride, a plot of the allyl chloride concentration versus the observed reaction rate constant (k_{obs}) should be linear (eq 4). The observed rate constant for a reaction following Path B need not be directly proportional to the allyl chloride concentration. The rate law for a reaction following this pathway is shown in eq 5. This equation indicates that if conditions can be found such that k_4[RCl] is not always much larger than k_{-3}[py], added py should

$$\text{rate} = \frac{k_3k_4[\text{RCl}][\mathbf{1}]}{k_{-3}[\text{py}] + k_4[\text{RCl}]} = k_{\text{obs}}[\mathbf{1}] \tag{5}$$

$$\frac{1}{k_{\text{obs}}} = \frac{1}{k_3} + \left(\frac{k_{-3}}{k_3k_4}\right)\left(\frac{[\text{py}]}{[\text{RCl}]}\right) \tag{6}$$

inhibit the reaction rate. Over a range of py and RCl concentrations, a plot of $1/k_{\text{obs}}$ versus the [py]/[RCl] ratio should be linear (eq 6).

Qualitatively, we observe that added pyridine does slow the rate of substitution. A plot of $1/k_{\text{obs}}$ versus [py]/[allyl chloride] is shown in Figure 3. The plot is linear, consistent with pyridine dissociation occurring prior to reaction of the Cp*$_2$Ti=S intermediate with allyl chloride (path B). The rate constant for pyridine dissociation from **1** at 20 °C can be determined from the value of the *y*-intercept of this plot, which is equal to $1/k_3$. This value is approximately 2.2×10^{-2} s^{-1}.

The fact that added pyridine retards the reaction rate of **1** with allyl chloride and benzyl chloride suggests that these transformations occur by reaction of the organic halide with the 16-electron Cp*$_2$Ti(S) fragment. This is significant because it implies that a reaction pathway in which C−Cl bond breaking is facilitated by interaction of the halide with the metal center is preferred over one in which **1** reacts directly with the electrophile. These conclusions are supported by the regioselectivity of the reaction of **1** with allyl chloride (vide infra).

As mentioned in the Results section, **1** reacts regioselectively with substituted allyl chlorides to form products resulting from S_N2' substitution of the halide anion. Exclusive S_N2' substitution of allyl halides is very rare, since this mode of substitution requires that the nucleophile attack a relatively electron-rich carbon center instead of the more electropositive α-carbon.[40] Many reactions once thought to occur via S_N2' processes have been shown to actually occur by reaction of the nucleophile with an allyl halide ion pair,[41] and it is difficult to find examples of nucleophiles that react exclusively via a S_N2' pathway when S_N2' substitution is sterically disfavored.[42] Various organometallic compounds have been shown to give some S_N2' substitution product when treated with allyl halides,[43] although to our knowledge RCu·BF$_3$ is a rare example of an organometallic reagent that reacts exclusively in an S_N2' manner.[44,45]

The appearance of S_N2' products in reactions of organometallic reagents with allyl halides is often explained by postulating an interaction between the metal center and the leaving group in a six-membered transition state.[43,46−49] It seems likely that substitution by the titanocene sulfido complex proceeds via a similar mechanism in which the halide leaving group interacts with the Cp*$_2$Ti(S) LUMO. A diagram of this postulated transition state is shown in Figure 7A. This mechanism is

(30) For other reactions illustrating the basic or nucleophilic properties of complexes containing metal−oxygen or metal−sulfur multiple bonds see refs 11 and 31−38. For a review of the nucleophilicity of metal−heteroatom bonds see: Caulton, K. G. *New J. Chem.* **1994**, *18*, 25.

(31) Pasini, A.; Colombo, A.; Marturano, G. *Polyhedron* **1995**, *15*, 481.

(32) Brunner, H.; Kubicki, M. M.; Leblanc, J. C.; Moise, C.; Volpato, F.; Wachter, J. *J. Chem. Soc., Chem. Commun.* **1993**, 851.

(33) Jernakoff, P.; Geoffroy, G. L.; Rheingold, A. L.; Geib, S. J. *J. Chem. Soc., Chem. Commun.* **1987**, 1610.

(34) Fischer, J.; Kress, J.; Osborn, J. A.; Ricard, L.; Westolek, M. *Polyhedron* **1987**, *6*, 1839.

(35) Bridgeman, A. J.; Davis, L.; Dixon, S. J.; Green, J. C.; Wright, I. N. *J. Chem. Soc., Dalton Trans.* **1995**, 1023.

(36) Pilato, R. S.; Housmekerides, C. E.; Jernakoff, P.; Rubin, D.; Geoffroy, G. L. *Organometallics* **1990**, *9*, 2333.

(37) Pilato, R. S.; Rubin, D.; Geoffroy, G. L.; Rheingold, A. L. *Inorg. Chem.* **1990**, *29*, 1986.

(38) Pilato, R. S.; Geoffroy, G. L.; Rheingold, A. L. *J. Chem. Soc., Chem. Commun.* **1989**, 1287.

(39) Theoretically, either pathway could occur via single electron transfer (SET) steps; however, the regioselectivity observed in reactions of **1** with substituted allyl chlorides indicates that in these reactions an SET mechanism is not operative. For an interesting study of electron-transfer reactions of a titanocene carbene complex see: Buchwald, S. L.; Ansyln, E. V.; Grubbs, R. H. *J. Am. Chem. Soc.* **1985**, *107*, 1766.

(40) Bordwell, F. G. *Acc. Chem. Res.* **1970**, *3*, 281.

(41) Bordwell, F. G.; Clemens, A. H.; Cheng, J.-P. *J. Am. Chem. Soc.* **1987**, *109*, 1773.

(42) Cyclobutenyl chlorides have been shown to undergo S_N2' reactions with NaOMe. See: Kirmse, W.; Scheidt, F.; Vater, H. J. *J. Am. Chem. Soc.* **1978**, *100*, 3945.

(43) Magid, R. M. *Tetrahedron* **1980**, *36*, 1901.

(44) Yamamoto, Y. *Angew. Chem., Int. Ed. Engl.* **1986**, *25*, 947.

(45) Yamamoto, Y.; Yamamoto, S.; Yatagai, H.; Maruyama, K. *J. Am. Chem. Soc.* **1980**, *102*, 2318.

(46) Magid, R. M.; Nieh, E. C.; Gandour, R. D. *J. Org. Chem.* **1971**, *36*, 2099.

(47) Lenox, R. S.; Katzenellenbogen, J. A. *J. Am. Chem. Soc.* **1973**, *95*, 957.

(48) Chaabouni, R.; Laurent, A.; Marquet, B. *J. Am. Chem. Soc.* **1976**, *98*, 757.

(49) Fraser-Reid, B.; Tam, S. Y. K.; Radatus, B. *Can. J. Chem.* **1975**, *53*, 2005.

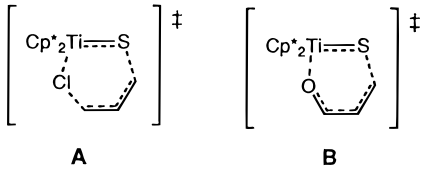

Figure 7. Postulated transition states for the reaction of **1** with allyl chlorides (A) and α,β-unsaturated aldehydes (B).

consistent with the observed pyridine inhibition of the reaction rate, since pyridine dissociation must precede interaction of the halide with the metal center. It should be noted that Parkin et al. have recently suggested that the deprotonation of acetone and ^{t}BuI by $Cp^*_2Zr(O)py$ may occur via similar transition states.[11]

This hypothesis also explains the different substitution regioselectivity (S_N2 rather than S_N2') observed when **1** reacts with allyl tosylate. Apparently, the tosylate moiety is unable to interact directly with the metal center in a transition state leading to S_N2' substitution, and so the lowest energy reaction pathway involves direct attack on the substituted carbon. The observation that the reaction of **1** with allyl tosylate is considerably slower than the reaction of **1** with allyl chloride, even though tosylates are generally more easily displaced than chlorides,[50,51] provides further evidence that these reactions do not proceed via the same mechanism.[52]

It is also possible that the reactions of **1** with α,β-unsaturated aldehydes occur via six-membered transition states (Figure 7B). In this case, the carbonyl functionality would interact with the metal center through one of the oxygen lone pairs. However, attack of "soft" nucleophiles at the β position of α,β-unsaturated aldehydes is much more common than S_N2' substitution of allyl halides, so the postulate of a concerted reaction proceeding via a six-membered transition state may not be necessary to explain the regioselectivity observed in these transformations.

Conclusion

We have shown that the (decamethylcyclopentadienyl)-titanium sulfido complex **1** undergoes regiospecific cycloaddition reactions with nitriles and terminal alkynes. These transformations are probably mediated by the vacant metal orbital adjacent to the sulfido ligand in the 16-electron Cp^*_2-Ti=S species. We have also found that **1** undergoes very regioselective nucleophilic substitution reactions with alkyl halides, alkyl tosylates, and α,β-unsaturated aldehydes. A kinetic study has established that the reaction of **1** with allyl chlorides involves initial reversible dissociation of pyridine. This is most likely followed by coordination of the halogen atom at the metal center and attack of the sulfur atom at the γ-carbon, leading to product via a six-membered transition state. In this way the vacant metal-based orbital also plays an important role in substitution reactions of these metal-heteroatom complexes.

(50) March, J. *Advanced Organic Chemistry*, 4th ed.; John Wiley & Sons: New York, 1992.

(51) Streitwieser, A. *Solvolytic Displacement Reactions*; McGraw-Hill: New York, 1962.

(52) The relative rates of the reactions of **1** with benzyl chloride and allyl tosylate suggest that benzyl chloride substitution also does not occur via a simple S_N2 mechanism. The rate of this reaction is inhibited by pyridine, indicating that halide dissociation might be assisted by coordination of the halide to the metal center in the transition state of the substitution. It is possible that formation of **9** occurs via Claisen-type attack of sulfur at the ortho position of the aromatic ring, followed by 1,3-migration to give the observed product. At this time we are unable to distinguish between this mechanism or other processes such as those proceeding via electron transfer.

Experimental Section

General Methods. Unless otherwise noted, all reactions and manipulations were carried out in dry glassware under a nitrogen or argon atmosphere using standard Schlenk techniques or at 20 °C in a Vacuum atmospheres 553-2 drybox equipped with a MO-40-2 inert gas purifier. The amount of O_2 in the drybox atmosphere was monitored with a Teledyne model no. 316 trace oxygen analyzer. Some reactions were carried out in thick-walled glass vessels fused to vacuum stopcocks. These vessels are referred to in the procedures as bombs. The other instrumentation and general procedures used have been described previously.[53]

Unless otherwise specified, all reagents were purchased from commercial suppliers and used without further purification. Pyridine was distilled sequentially from CaH_2 and sodium and was stored over activated 4 Å molecular sieves. Sulfur was dissolved in dry benzene containing activated 4 Å molecular sieves, stirred overnight, and then recrystallized from the filtered benzene solution. Pentane and hexane (UV grade) were distilled from sodium benzophenone ketyl/tetraglyme under nitrogen. Deuterated solvents for NMR experiments were dried in the same way as their protiated analogues but were vacuum transferred from the drying agent. Acetylene was bubbled through concentrated H_2SO_4 and passed through two −78 °C cold traps. Methyl iodide, phenylacetylene, tolylacetylene, nitriles, α,β-unsaturated aldehydes, allyl fluoride, and all allyl chlorides were dried over activated 4 Å molecular sieves before use. $Cp^*_2Ti(C_2H_4)$ was prepared by the literature method, except that Cp^*_2TiCl was used instead of $Cp^*_2TiCl_2$.[54] 3-Chloro-3-methylbut-1-ene,[55] allyl tosylate, and allyl tosylate-1-*d*[56] were prepared according to literature procedures.

The HMQC experiment was recorded on a Brucker AMX spectrometer resonating at 300.13 MHz for ^{1}H and 75.42 MHz for ^{13}C that was equipped with an inverse probe. One-dimensional NMR spectra were recorded on the Brucker AMX spectrometer described above or on a Brucker AMX spectrometer resonating at 400 MHz for ^{1}H and 100 MHz for ^{13}C that was equipped with a QNP probe. ^{1}H and ^{13}C-{^{1}H} NMR spectra were referenced to resonances corresponding to residual protons or carbon atoms of the solvent. ^{19}F NMR spectra were externally referenced to CCl_3F ($\delta = 0.0$ ppm).

$Cp^*_2Ti(=S)py$ (1). A solution of $Cp^*_2Ti(CH_2CH_2)$ (486 mg, 1.40 mmol) and pyridine (0.56 mL, 5 equiv) in toluene (20 mL) was cooled to −40 °C. To this stirred solution, a suspension of freshly recrystallized sulfur (33 mg, 1.0 equiv) in cold toluene was added dropwise. The green solution immediately turned dark. After 40 h, the solvent was reduced in vacuo (to approximately 10 mL) and pentane was layered onto the toluene solution. This mixture was cooled to −40 °C to yield **1** as red crystals (459 mg, 76%). ^{1}H NMR (C_6D_6): δ 8.00 (d, 2H), 6.64 (m, 1H), 6.25 (m, 2H), 1.90 (s, 30H) ppm. ^{13}C NMR: δ 135.9 (CH), 128.3 (CH), 122.4 (CH), 120.3 ($C{-}CH_3$), 13.3 ($C{-}CH_3$) ppm. IR (Nujol): 2730, 1598, 1209, 1014, 802, 755, 709 cm^{-1}. MS (EI): *m*/*z* 430 (M^+). Anal. Calcd for $C_{25}H_{35}NSTi$: C, 69.90; H, 8.22; N, 3.26. Found: C, 69.88; H, 8.25; N, 3.23.

$Cp^*_2Ti(SC(H)CH)$ (2). A bomb was charged with **1** (95 mg, 0.22 mmol) dissolved in benzene (10 mL). Acetylene was bubbled through the solution for 5 min, and the resulting mixture was allowed to stand overnight. The solution was filtered several times through fiberglass filter paper, and the volatile materials were removed in vacuo. Crystallization of the residue from a toluene/hexane solution at −40 °C gave 52 mg (62%) of **2** as brown crystals. ^{1}H NMR (C_6D_6): δ 7.42 (d, $J = 9.9$ Hz, 1H), 6.95 (d, $J = 9.9$ Hz, 1H), 1.69 (s, 30H) ppm. ^{13}C NMR: δ 194.9 (CH), 120.0 ($C{-}CH_3$), 96.5 (CH), 11.8 ($C{-}CH_3$) ppm. IR (Nujol): 2723, 1490, 1446, 1187, 1020, 806, 673 cm^{-1}. MS (EI): *m*/*z* 376 (M^+). Anal. Calcd for $C_{22}H_{32}STi$: C, 70.20; H, 8.57. Found: C, 70.10; H, 8.67.

$Cp^*_2Ti(SC(Ph)CH)$ (3). A Schlenk flask equipped with a Teflon stir bar was charged with **1** (51 mg, 0.12 mmol) dissolved in benzene

(53) Meyer, K. E.; Walsh, P. J.; Bergman, R. G. *J. Am. Chem. Soc.* **1995**, *117*, 3749.

(54) Cohen, S. A.; Auburn, P. R.; Bercaw, J. E. *J. Am. Chem. Soc.* **1983**, *105*, 1136.

(55) Sneen, R. A.; Key, P. S. *J. Am. Chem. Soc.* **1972**, *94*, 6983.

(56) Baldwin, J. E.; Bradley, M.; Turner, N. J.; Adlington, R. M.; Pitt, A. R.; Sheridan, H. *Tetrahedron* **1991**, *47*, 8203.

(5 mL). Phenylacetylene (80 μL, 0.72 mmol) was dissolved in benzene (2 mL), and the solutions were combined. The reaction mixture was stirred overnight, and the volatile materials were removed to yield 52.1 mg of analytically pure **3** (95%). ^{1}H NMR (C_6D_6): δ 8.06 (m, 2H), 7.80 (s, 1H), 7.27 (m, 2H), 7.11 (m, 1H), 1.69 (s, 30H) ppm. ^{13}C NMR: δ 191.4 (CH), 137.5 (C), 128.2 (CH), 126.6 (CH), 126.4 (*C*−CH_3), 122.0 (CH), 115.3 (C), 12.1 (C−*C*H_3) ppm. IR (Nujol): 3100, 2717, 1968, 1874, 1789, 1737, 1164, 1020, 904, 730 cm^{-1}. MS (EI): *m*/*z* 452 (M^+). Anal. Calcd for $C_{28}H_{36}STi$: C, 74.32; H, 8.02. Found: C, 74.35; H 8.02.

Cp*$_2$Ti(SC(Tol)CH) (4). A scintillation vial was charged with **1** (122 mg, 0.28 mmol) in benzene (5 mL). *p*-Tolylacetylene (165 mg, 1.4 mmol) was added via syringe, and the solution was stirred at RT (room temperature) for 2 d. The volatile materials were removed, and the remaining solid was crystallized from a toluene/pentane mixture at −40 °C to yield **4** as dark orange crystals (98 mg, 74%). ^{1}H NMR (C_6D_6): δ 7.98 (d, 2H, J = 8.0 Hz), 7.79 (s, 1H), 7.10 (d, 2H, J = 8.0 Hz), 1.80 (s, 3H), 1.70 (s, 30 H) ppm. ^{13}C NMR: δ 190.3 (CH), 135.4 (C), 134.5 (C), 129.0 (CH), 126.3 (CH), 121.7 (*C*−CH_3), 114.8 (CH), 20.8 (CH_3), 11.9 (C−*C*H_3) ppm. IR (Nujol): 3020, 2713, 1565, 1506, 1118, 1020, 817, 757, 636 cm^{-1}. MS (EI): *m*/*z* 466 (M^+). Anal. Calcd for $C_{29}H_{38}STi$: C, 74.66; H, 8.21. Found: C, 74.31; H, 8.13.

Cp*$_2$Ti(SC(SiMe$_3$)CH) (5). A scintillation vial was charged with a solution of **1** (110 mg, 0.26 mmol) in benzene (5 mL). (Trimethylsilyl)acetylene (150 mg, 1.5 mmol) was added via syringe. The reaction mixture was allowed to stir for 3 d. The volatile materials were removed, and crystallization of the residue from pentane at −40 °C gave **5** as large orange crystals (98 mg, 85%) ^{1}H NMR (C_6D_6): δ 8.20 (s, 1H), 1.66 (s, 30H), 0.47 (s, 9H) ppm. ^{13}C NMR: δ 210.4 (CH), 118.9 (*C*−CH_3), 97.6 (C), 12.4 (C−*C*H_3), 1.2 (CH_3) ppm. IR (cyclohexane): 3008, 1498, 1459, 1373, 1240, 831, 742 cm^{-1}. MS (EI): *m*/*z* 448 (M^+). Anal. Calcd for $C_{25}H_{40}SSiTi$: C, 66.93; H, 8.99. Found: C, 66.88; H, 9.07.

Cp*$_2$Ti(SC(Ph)N) (6). A scintillation vial was charged with **1** (192 mg, 0.45 mmol) in benzene (5 mL). Benzonitrile (46 μL, 0.45 mmol) was added via syringe. After 2 h, the volatile materials were removed to give an orange solid that was recrystallized from toluene/pentane at −40 °C to yield **6** (132 mg, 65%) as orange crystals. ^{1}H NMR (C_6D_6): δ 8.47 (m, 2H), 7.27 (t, 2H), 7.14 (m, 1 H), 1.72 (s, 30H) ppm. ^{13}C NMR: δ 143.9 (C), 137.7 (C), 129.0 (CH), 128.3 (CH), 125.4 (CH), 123.1 (*C*−CH_3), 11.8 (C−*C*H_3) ppm. IR (Nujol): 3020, 2730, 2036, 1882, 1818, 1641, 1454, 1375, 1155, 1066, 881, 759, 692, 609 cm^{-1}. MS (EI): *m*/*z* 454 (M + H^+). Anal. Calcd for $C_{27}H_{35}$-NSTi: C, 71.51; H, 7.78; N, 3.09. Found: C, 71.38; H, 7.84; N, 3.15.

Cp*$_2$Ti(SC(*m*-Tol)N) (7). A scintillation vial was charged with **1** (103 mg, 0.24 mmol) in benzene (5 mL). *m*-Tolunitrile (29 uL, 0.24 mmol)) was added via syringe. After 6 h, the volatile materials were removed to give an orange solid that was crystallized from toluene/pentane at −40 °C to yield 73 mg of **7** (56%) as an orange powder. ^{1}H NMR (C_6D_6): δ 8.52 (m, 1H), 7.34 (t, 1H), 7.15 (m, 1H), 6.97 (d, 1H), 2.16 (s, 3H), 1.73 (s, 30H). ^{13}C NMR: δ 143.9 (C), 137.8 (C), 137.4 (CH), 129.8 (CH), 128.8 (CH), 124.8 (CH), 123.0 (*C*−CH_3), 21.2 (CH_3), 11.8 (C−*C*H_3) ppm. IR (Nujol): 3045, 2719, 1795, 1619, 1020, 929, 784, 692, 559 cm^{-1}. MS (EI): *m*/*z* 468 (M + 1). Anal. Calcd for $C_{28}H_{37}NSTi$: C, 71.93; H, 7.98; N, 3.00. Found: C, 71.80; H, 7.86; N, 2.76.

Cp*$_2$Ti(I)SMe (8). A bomb was charged with **1** (135 mg, 0.31 mmol) in benzene (5 mL). Methyl iodide (0.35 mmol) was vacuum transferred onto the frozen solution at −196 °C. The solution turned green after standing for 5 min at RT. After 12 h, the volatile materials were removed to yield a green solid. This material was crystallized from toluene/pentane at −40 °C to give 86 mg of **8** (55%) as a green solid. ^{1}H NMR (C_6D_6): 2.89 (s, 3H), 1.94 (s, 30H) ppm. ^{13}C NMR: δ 125.2 (*C*−CH3) 28.3 (*C*H3), 14.2 (C−*C*H_3) ppm. IR (Nujol): 2721, 1544, 1308, 1018, 582 cm^{-1}. MS (EI) *m*/*z* 492 (M^+). Anal. Calcd for $C_{21}H_{33}ISTi$: C, 51.23; H, 6.75. Found: C, 51.23; H, 6.76.

Cp*$_2$Ti(Cl)SCH$_2$Ph (9). Benzyl chloride (29 μL, 0.25 mmol) was added via syringe to a stirred solution of **1** (100 mg, 0.23 mmol) in benzene (5 mL). After 5 min the color of the solution had changed from red to purple. The reaction mixture was allowed to stir for 30 min, and the volatile materials were removed. The remaining solid was crystallized from toluene at −40 °C to yield 87 mg of **9** (78%) as blue crystals.^{1}H NMR (C_6D_6): δ 7.48 (m, 2H), 7.01 (m, 3H), 4.32 (s, 2H), 1.88 (s, 30H) ppm. ^{13}C NMR: δ 144.8 (CH), 129.2 (C), 128.7 (CH), 126.0 (CH), 125.4 (*C*−CH_3), 48.7 (CH_2), 12.8 (C−*C*H_3) ppm. IR (Nujol): 3058, 2707, 1598, 1492, 1218, 1182, 1066, 1020, 707 cm^{-1}. MS (EI) *m*/*z* 476 (M^+) Anal. Calcd for $C_{27}H_{37}ClSTi$: C, 67.99; H, 7.82. Found: C, 67.89; 7.64.

Cp*$_2$Ti(Cl)SCH$_2$CHCH$_2$ (10). A bomb containing a frozen solution of **1** (164 mg, 0.38 mmol) in benzene was evacuated, and 1.5 equiv (0.57 mmol) of 3-chloropropene was condensed onto the frozen solution at −196 °C. Upon thawing, the solution color changed immediately from red to green. The solution was allowed to stand for 2 h, and the volatile materials were removed. The resulting green solid was recrystallized from ether/pentane at −40 °C to yield **10** as purple crystals (99 mg, 61%). ^{1}H NMR (C_6D_6): δ 6.13 (m, 1H), 5.19 (m, 1H), 4.95 (m, 1H), 3.76 (m, 2H), 1.88 (s, 30H) ppm. ^{13}C NMR: δ 139.0 (CH), 125.3 (*C*−CH_3, 113.3 (CH), 47.0 (CH_2), 12.7 (C−*C*H_3) ppm. IR (Nujol): 3054, 2719, 1631, 1209, 1072, 1018, 917, 744 cm^{-1}. MS (EI): *m*/*z* 426 (M^+). Anal. Calcd for $C_{23}H_{35}ClSTi$: C, 64.71; H, 8.26. Found: C, 64.74; H, 8.28.

Cp*$_2$Ti(Cl)SCH$_2$CHCHCH$_3$ (11). A bomb containing a frozen solution of **1** (151 mg, 0.35 mmol) in benzene was evacuated, and 1.1 equiv (0.39 mmol) of 3-chloro-1-butene was condensed in at −196 °C. Upon thawing, the solution color changed immediately from red to green. The solution was allowed to stand for several hours. The volatile materials were removed to give a green solid that was crystallized from toluene/pentane at −40 °C to give **11** as a blue, crystalline solid (120 mg, 77%). ^{1}H NMR (C_6D_6): δ 5.77 (m, 1H), 5.56 (m, 1H), 3.74 (m, 2H), 1.90 (s, 30H), 1.59 (d, J = 6.4 Hz, 3H) ppm. ^{13}C NMR: δ 132.1 (CH), 125.2 (*C*−CH_3), 124.2 (CH), 46.6 (CH), 17.7 (CH_3), 12.7 (C−*C*H_3) ppm. IR (Nujol): 3067, 2719, 1195, 1020, 960, 809, 694 cm^{-1}. MS (EI): *m*/*z* 440 (M^+). Anal. Calcd for $C_{24}H_{37}ClSTi$: C, 65.37; H, 8.46. Found: C, 65.40; H, 8.63.

Cp*$_2$Ti(Cl)SCH(CH$_3$)CHCH$_2$ (12). A bomb containing a frozen solution of **1** (151 mg, 0.27 mmol) in benzene was evacuated, and 1 equiv of crotyl chloride (0.27 mmol) was condensed into the bomb at −196 °C. Upon thawing, the solution color changed immediately from red to green. The reaction mixture was allowed to stand for 2 h. The volatile materials were removed to yield a green solid that was crystallized from ether at −40 °C to yield 121 mg (77%) of **12** as blue crystals. ^{1}H NMR (C_6D_6): δ 6.45 (m, 1H), 5.31 (m, 1H), 5.08 (m, 1H), 4.32 (m, 2H), 1.90 (s, 15H), 1.88 (s, 15H), 1.65 (d, J = 6.8 Hz, 3H) ppm. ^{13}C NMR: δ 144.4 (CH), 125.3 (*C*−CH_3), 110.1 (CH_2), 48.1 (CH), 21.3 (CH_3), 12.9 (C−*C*H_3), 12.9 (C−*C*H_3) ppm. IR (cyclohexane): 3087, 2732, 1635, 1498, 1378, 1029, 809, 727, 690 cm^{-1}. Anal. Calcd for $C_{24}H_{37}ClSTi$: C, 65.37; H, 8.46. Found: C, 65.60; H, 8.59.

Cp*$_2$Ti(Cl)SCH$_2$CHC(CH$_3$)$_2$ (13). To a vial containing a stirred solution of **1** (186 mg, 0.43 mmol) in benzene was added 3-chloro-3-methylbut-1-ene (55 μL, 0.52 mmol) via syringe. The solution color immediately changed from red to green. The solution was stirred for 30 min, and then the volatile materials were removed to give a green-blue solid that was recrystallized from ether at −40 °C to give **13** as blue crystals (131 mg, 70%). ^{1}H NMR (C_6D_6): δ 5.66 (m, 1H), 3.80 (d, J = 7.9 Hz, 2H), 1.90 (s, 30H), 1.70 (s, 3H), 1.66 (s, 3H). ^{13}C NMR: δ 131.3 (C), 126.4 (CH), 125.4 (*C*−CH_3), 43.1 (CH_2), 25.8 (CH_3), 18.2 (CH_3), 13.0 (C−*C*H_3) ppm. IR (Nujol): 3021, 2719, 1666, 1199, 1103, 1018, 848 cm^{-1}. Anal. Calcd for $C_{25}H_{39}ClSTi$: C, 66.00; H, 8.64. Found: C, 65.83; H, 8.64.

Cp*$_2$Ti(Cl)SC(CH$_3$)$_2$CHCH$_2$ (14). Neat 1-chloro-3-methyl-2-butene (105 μL, 0.93 mmol) was added to a solution of **1** (100 mg, 0.23 mmol) in C_6H_6 (5 mL). The reaction mixture was agitated and then allowed to stand for 15 min. The volatile materials were removed, and the remaining solid was crystallized from toluene/pentane at −40 °C to yield **14** as large blue crystals (57 mg, 54%). ^{1}H NMR (C_6D_6): δ 6.63 (m, 1H), 5.10 (m, 1H), 4.98 (m, 1H), 1.89 (s, 30H), 1.68 (s, 6H) ppm. ^{13}C NMR: δ 151.4 (CH), 127.1 (*C*−CH_3), 107.5 (CH_2), 55.5 (C), 33.1 (CH_3), 13.4 (*C*−*C*H_3) ppm. IR (Nujol): 2709, 1625, 1376, 1105, 1014, 904, 794, 694, 592 cm^{-1}. MS (EI): *m*/*z* 454 (M^+). Anal. Calcd for $C_{25}H_{39}ClSTi$: C, 66.00; H, 8.64. Found: C, 65.91; H, 8.64.

Cp*$_2$Ti(Cl)SCH(CHCH$_2$)CHCH$_2$ (15). 5-Chloro-1,3-pentadiene (30 μL, 0.27 mmol) was added to a solution of **1** (98 mg, 0.23 mmol) in benzene (7 mL). The reaction mixture was stirred for 4 h. The volatile materials were removed, and the remaining solid was crystallized from Et$_2$O/pentane at −40 °C to yield **15** as a dark green solid (68 mg, 65%). ^{1}H NMR (C_6D_6): δ 6.22 (m, 2H), 5.24 (m, 2H), 5.08 (m, 2H), 4.64 (m, 1H), 1.88 (s, 30H) ppm. ^{13}C NMR: δ 140.5 (CH), 125.8 (C−CH$_3$), 112.8 (CH$_2$), 55.5 (CH), 13.15 (C−CH$_3$) ppm. IR (C_6D_6): 2983, 2718, 1631, 1525, 1390, 911, 773. Anal. Calcd for $C_{25}H_{37}ClSTi$: C, 66.30; H, 8.23. Found: C, 66.12; H, 8.32.

Cp*$_2$Ti(F)CH$_2$CHCH$_2$ (16). 3-Fluoropropene (0.63 mmol) was condensed into a bomb containing a frozen benzene solution of **1** (90 mg, 0.21 mmol). The solution was thawed and was allowed to stand for 5 h. The volatile materials were removed to give a red solid that was crystallized from ether/pentane at −40 °C to give **16** as dark red crystals (49 mg, 54%). ^{1}H NMR (C_6D_6): δ 6.16 (m, 1H), 5.22 (m, 1H), 4.98 (m, 1H), 3.52 (m, 2H), 1.84 (s, 30H) ppm. ^{13}C NMR: δ 139.8 (CH), 124.1 (*C*−CH$_3$), 112.6 (CH$_2$), 41.9 (d, CH, J_{CF} = 7 Hz), 11.7 (C−*C*H$_3$) ppm. ^{19}F NMR: δ 20.4 ppm. IR (Nujol): 3072, 2719, 1629, 1207, 1019, 907, 734 cm^{-1}. Anal. Calcd for $C_{23}H_{35}FSTi$: C, 67.30; H, 8.59. Found: C, 67.10; H, 8.58.

Cp*$_2$Ti(Br)SCH$_2$CHCH$_2$ (17). 3-Bromopropene (26 μL, 0.29 mmol) was added via syringe to a vial containing a stirred solution of **1** (115 mg, 0.26 mmol) in benzene (5 mL). The solution color changed from red to green, and the solution was allowed to stir for 10 min. The volatile materials were removed to give a blue-green solid that was crystallized from ether/pentane at −40 °C to give **17** as dark blue crystals (85 mg, 67%). ^{1}H NMR (C_6D_6): δ 6.13 (m, 1H), 5.18 (m, 1H), 4.95 (m, 1H), 3.82 (m, 2H), 1.91 (s, 30H) ppm. ^{13}C NMR: δ 138.7 (CH), 125.4 (*C*−CH$_3$), 113.4 (CH$_2$), 48.2 (CH$_2$), 13.1 (C−*C*H$_3$) ppm. IR (Nujol): 3091, 2717, 1633, 1198, 1018, 908, 808, 732 cm^{-1}. Anal. Calcd for $C_{23}H_{35}BrSTi$: C, 58.61; H, 7.48. Found: C, 58.61; H, 7.70.

Cp*$_2$Ti(I)SCH$_2$CHCH$_2$ (18). 3-Iodopropene (18 μL 0.20 mmol) was added via syringe to a vial containing a stirred solution of **1** (80 mg, 0.19 mmol) in benzene (5 mL). The solution color changed from red to green, and the solution was allowed to stir for 10 min. The volatile materials were removed to give a blue-green solid that was crystallized from ether/pentane at −40 °C to give **18** as dark blue crystals (71 mg, 73%). ^{1}H NMR (C_6D_6): δ 6.15 (m, 1H), 5.18 (m, 1H), 4.95 (m, 1H), 3.90 (m, 2H), 1.97 (s, 30H) ppm. ^{13}C NMR: δ 138.7 (CH), 125.4 (*C*−CH$_3$), 113.9 (CH$_2$), 49.6 (CH$_2$), 14.2 (C−*C*H$_3$) ppm. IR (Nujol): 3079, 2704, 1631, 1199, 1020, 908, 742, 594 cm^{-1}. Anal. Calcd for $C_{23}H_{35}ISTi$: C, 53.29; H, 6.81. Found: C, 53.07; H, 6.81.

Cp*$_2$Ti(OSO$_2$Tol)SCH$_2$CHCH$_2$ (19). Allyl tosylate (57 μL, 0.30 mol) was added to a vial containing a stirred solution of **1** (119 mg, 0.28 mmol) in benzene (10 mL). The solution was stirred for 3 d at 20 °C. The volatile materials were removed to give a brown oily solid that was washed with 5 mL of Et$_2$O and pentane to give **19** as a brown solid (87 mg, 56%). ^{1}H NMR (C_6D_6): δ 7.97 (d, 2H, J = 8.1 Hz), 6.89 (d, 2H, J = 8.0 Hz), 6.45 (m, 1H), 5.35 (m, 1H), 5.10 (m, 1H), 4.72 (m, 2H), 1.96 (s, 3H), 1.90 (s, 30H) ppm. ^{13}C NMR: δ 143.9 (C), 140.3 (C), 140.2 (CH), 128.8 (CH), 127.4 (*C*−CH$_3$), 127.3 (CH), 114.5 (CH$_2$), 44.1 (CH$_2$), 21.1 (CH$_3$), 13.0 (C−*C*H$_3$) ppm. IR (C_6H_6): 2900, 2829, 1783, 1670, 1396, 1164, 1058, 874, 858 cm^{-1}. Anal. Calcd for $C_{30}H_{42}S_2O_3Ti$: C, 64.04; H, 7.52. Found: C, 64.28; H, 7.85. The ^{2}H NMR spectra of the ^{2}H-substituted analogue (which was prepared using 56 mg of **1** and the procedures described above) in C_6H_6 showed only a singlet at 4.7 ppm. The ^{13}C{^{1}H} spectrum of this compound was identical to that of the undeuterated analogue except the singlet at 44 ppm was replaced by a 1:1:1 triplet.

Cp*$_2$TiSCH(CH$_3$)C(CH$_3$)CHO (20). *trans*-2-Butenal (50 mg, 0.52 mmol) was added via syringe to a stirred solution of **1** (150 mg, 0.35 mmol) in benzene. After 2 h the volatile materials were removed and the remaining brown solid was crystallized from a toluene/pentane solution at −40 °C to give 128 mg of **20** (84%) as a purple solid. ^{1}H NMR (C_6D_6): δ 7.25 (s, 1H), 4.15 (q, J = 6.3 Hz, 1H), 1.89 (s, 15H), 1.85 (s, 15H), 1.70 (d, J = 6.3 Hz, 3 H), 1.67 (s, 3H) ppm. ^{13}C NMR: δ 157.5 (CH), 122.0 (*C*−CH$_3$), 43.2 (CH), 27.3 (CH$_3$), 16.1 (CH$_3$), 12.8 (C−*C*H$_3$), 12.5 (C−*C*H$_3$) ppm. IR (Nujol): 2723, 1687, 1612, 1214, 1159, 1020, 846, 653 cm^{-1}. MS (EI): *m*/*z* 434 (M$^+$). Anal. Calcd for $C_{25}H_{38}OSTi$: C, 69.11; H, 8.81. Found: C, 69.14; H, 8.79.

Cp*$_2$TiSCH(Ph)C(CH$_3$)CHO (21). A small scintillation vial was charged with a solution of **1** (148 mg, 0.36 mmol) in 5 mL of benzene. α-Methyl-*trans*-cinnamaldehyde (72 μL, 0.52 mmol) was added via syringe, and the solution was agitated with a pipet. After 30 min, the volatile materials were removed, and the resulting green oil was crystallized from pentane at −40 °C to give 70 mg of **21** (41%). ^{1}H NMR (C_6D_6): δ 7.63 (m, 2H), 7.29 (s, 1H), 7.24 (t, 2H), 7.09 (t, 1H), 5.18 (s, 1H), 1.90 (s, 15H), 1.85 (s, 15H), 1.43 (s, 3H) ppm. ^{13}C NMR: δ 158.3 (*C*(O)(H)), 146.6 (C), 129.5 (CH), 127.8 (CH), 126.7 (CH). 124.3 (*C*−CH$_3$), 123.6 (*C*−CH$_3$), 106.0 (C), 53.3 (CH), 17.5 (CH$_3$), 12.3 (C−*C*H$_3$), 11.9 (C−*C*H$_3$) ppm. IR (cyclohexane): 3064, 3029, 2950, 2732, 1614, 1380, 1211, 1174, 709, 611 cm^{-1}. MS (EI): *m*/*z* 496 (M$^+$). Anal. Calcd for $C_{30}H_{40}OSTi$: C, 72.56; H, 8.12. Found: C, 72.68; H, 7.94.

X-ray Crystallographic Study of Cp*$_2$Ti(SC(SiMe$_3$)CHCH$_2$) (5). Crystals of **5** suitable for X-ray diffraction were obtained by slow cooling of a pentane solution of **5** to −40 °C. A fragment of one of these reddish lumps with the approximate dimensions of 0.15 × 0.20 × 0.27 mm was mounted on a glass fiber using Paratone N hydrocarbon oil. All measurements were made on a Siemens SMART diffractometer with a CCD area detector using graphite-monochromated Mo Kα radiation. All calculations were performed using the TEXSAN crystallographic software package.

Cell constants and an orientation matrix obtained from a least-squares refinement using the measured positions of 4907 reflections in the range $3.00 < 2\theta < 45.00°$ corresponded to a primitive monoclinic cell with dimensions given in the Supporting Information. The final cell parameters and specific data collection parameters for this data set are given in Table 1 or as Supporting Information. The systematic absences of *h*01, *l* ≠ 2*n*, and 0*k*0, *k* ≠ 2*n*, uniquely determined the space group to be $P2_1/c$ (No. 14). Data were collected at a temperature of −100 ± 1 °C.

Data were integrated using SAINT with box parameters of 2.0 × 2.0 × 0.6 deg to a maximum 2θ values of 51.7°. The data were corrected for Lorentz and polarization effects. No decay correction was applied. An empirical absorption correction based on the measurement of redundant and equivalent reflections and an ellipsoidal model for the absorption surface was applied using XPREP (T_{max} = 0.90, T_{min} = 0.83). The 11 074 integrated reflections were averaged to yield 4534 unique reflections (R_{int} = 0.042). The structure was solved by direct methods and expanded using Fourier techniques. All non-hydrogen atoms were refined anisotropically. Hydrogen atoms were included at calculated or in located positions but not refined. The final cycle of full matrix least-squares refinement was based on 2713 observed reflections ($I > 3.00\sigma(I)$) and 253 variable parameters and converged (largest parameter shift was 0.01 times its esd) with unweighted and weighted agreement factors of R = 0.049 and R_w = 0.056. The standard deviation of an observation of unit weight was 1.89. The weighting scheme was based on counting statistics and included a factor (p = 0.030) to downweight the intense reflections. The maximum and minimum peaks on the final difference Fourier map corresponded to 0.77 and −0.55 e/Å^3, respectively.

X-ray Crystal Structure of Cp*$_2$Ti(Cl)SC(CH$_3$)$_2$CHCH$_2$ (14). Green crystals of **14** suitable for X-ray diffraction were grown by slow cooling of a toluene/pentane solution of **14** to −40 °C. A block-shaped crystal having approximate dimensions of 0.10 × 0.11 × 0.17 mm was mounted as described above. Data collection and calculations were also performed as described above. The specific data collection parameters are given in Table 1 or as Supporting Information. The space group was determined to be $P2_1/c$ (No. 14). Cell constants and an orientation matrix were obtained from 4509 reflections. Data were integrated as described above using box parameters of 1.6 × 1.6 × 0.6 deg to a maximum 2θ value of 52.1°. The 11 366 integrated and corrected reflections were averaged to yield 4378 unique data (R_{int} = 0.057). The final cycle of full-matrix least-squares refinement was based on 2416 observed reflections and converged (largest parameter shift was 0.45 times its esd) with unweighted and weighted agreement factors of R = 0.049 and R_w = 0.055. The standard deviation of an observation of unit weight was 1.65 using the weighting scheme

described above. The maximum and minimum peaks on the final difference Fourier map corresponded to 0.36 and −0.36 e/Å^3. All non-hydrogen atoms were refined anisotropically. Hydrogen atoms were included at calculated or in located positions but not refined.

X-ray Crystal Structure of Cp*$_2$Ti(SCH(Ph)C(Me)CHO) (21). Black crystals of **21** suitable for X-ray diffraction were grown by slow cooling of a toluene/pentane solution of **21** to −40 °C. A fragment of a block-shaped crystal having approximate dimensions of 0.16 × 0.18 × 0.21 mm was mounted as described above. Data collection and calculations were performed as described for the X-ray analysis of **5**. The space group was determined to be $P2_1/c$ (No. 14). The specific data collection parameters are given in Table 1 or as Supporting Information. Cell constants and an orientation matrix were obtained from 6064 reflections. Data were integrated as described above using box parameters of 1.8 × 1.8 × 0.6 deg to a maximum 2θ value of 46.5 °. The 10 623 integrated and corrected reflections were averaged to yield 3989 unique data ($R_{int} = 0.038$). The final cycle of full-matrix least-squares refinement was based on 2635 observed reflections and converged (largest parameter shift was 0.02 times its esd) with unweighted and weighted agreement factors of $R = 0.033$ and $R_w = 0.040$. The standard deviation of an observation of unit weight was 1.47 using the weighting scheme described above. The maximum and minimum peaks on the final difference Fourier map corresponded to 0.36 and −0.20 e/Å^3. All non-hydrogen atoms were refined anisotropically. Hydrogen atoms were included at calculated or in located positions but not refined.

Acknowledgment. We thank the National Institutes of Health for generous financial support of this work (Grant No. GM-25459 to R.G.B.), Dr. F. J. Hollander for solving the crystal structures of **5** and **21**, Dr. Ryan Powers for solving the crystal structure of **14** (both at CHEXRAY, the U. C. Berkeley X-ray diffraction facility), and a reviewer for a careful reading of the manuscript.

Supporting Information Available: Tables giving details of the data collection, data reduction, and structure solution and refinement, positional and thermal parameters, bond lengths, bond angles, and torsion angles for **5**, **14**, and **21** and a table and figure presenting data from the kinetic study of the reaction between **1** and allyl chloride (22 pages, print/PDF). See any current masthead page for ordering information and Web access instructions.

JA980877M